Content

Table S1 Crystal data and structure refinement parameters of **1**.

	1
Formula	$C_{22}H_{20}N_4O_6Co$
Formula weight	495.35
Crystal system	monoclinic
Space group	*C*2/*c*
a (Å)	11.280(2)
b (Å)	18.471(3)
c (Å)	20.171(4)
α (º)	90
β (º)	100.516(2)
γ (º)	90
Volume (Å^3)	4132.1(13)
Z	8
T (K)	296(2)
D_{calcd} (mg·m^{-3})	1.592
μ (mm^{-1})	0.881
R_{int}	0.0245
F(000)	2040
θ range (º)	$2.054 \leq \theta \leq 26.000$
Reflns. collected	21344
Data / restraints / parameters	4067/0/293
Goodness of fit on F^2	0.927
Final *R* indices [$I > 2\sigma(I)$]	R_1=0.0297, wR_2=0.0855
R indices (all data)	R_1=0.0346, wR_2=0.0883
Largest diff. peak and hole (e Å^{-3})	0.53 and -0.67

$R_1 = \Sigma| |F_o|-|F_c| |/\Sigma|F_o|$. $\omega R_2 = \Sigma[w(F_o^2-F_c^2)^2]/\Sigma[w(F_o^2)^2]^{1/2}$

Table S2 Selected bond lengths (Å) and angles (°) for **1**.

1			
Co(1)-N(1)	2.0751(15)	Co(1)-N(2C)	2.0596(16)
Co(1)-O(1B)	2.0366(14)	Co(1)-O(2B)	2.2958(15)
Co(1)-O(3A)	2.0161(15)	Co(1)-O(4A)	2.6001(15)
N(1)-Co(1)-O(2B)	91.31(6)	O(3A)-Co(1)-O(2B)	90.05(6)
N(1)-Co(1)-N(2C)	97.23(6)	O(1B)-Co(1)-O(2B)	60.24(5)
N(1)-Co(1)-O(3A)	99.88(6)	O(1B)-Co(1)-N(2C)	102.45(6)
O(3A)-Co(1)-N(2C)	103.21(7)	N(1)-Co(1)-O(2B)	114.38(6)
N(2C)-Co(1)-O(2B)	162.68(5)	O(3A)-Co(1)-O(1B)	133.61(6)

Symmetry codes: A: –1/2+x, 1/2–y, –1/2+z; B: –1+x, y, z; C: 1–x, –y, 1–z.

Table S3 Standard deviation and detection limit calculation for Fe^{3+}, $Cr_2O_7^{2-}$, CrO_4^{2-} and NFT.

	Fe^{3+}	$Cr_2O_7^{2-}$	CrO_4^{2-}	NFT
1	776.745189	794.583227	797.843189	793.831114
2	776.945375	794.633116	797.943267	793.974444
3	777.035281	794.493031	797.764316	793.716773
4	776.645356	794.715633	797.953343	793.962235
5	776.865284	794.423116	797.653377	793.753454
Standard deviation (σ)	0.13892	0.10283	0.11289	0.10534
Slope (m)	1.03×10^4	1.41×10^4	1.65×10^4	3.11×10^4
Detection limit (3σ/m)	4.04×10^{-5}	2.18×10^{-5}	2.05×10^{-5}	1.02×10^{-5}

Table S4 HOMO and LUMO energy levels of selected antibiotics and H_2DCB calculated by density functional theory (DFT) at $B_3LYP/6\text{-}31G^{**}$ level.

	HOMO (eV)	**LUMO (eV)**	**Band Gap (eV)**
NFT	-6.70	-3.12	3.58
CAP	-7.24	-2.52	4.72
DTZ	-6.93	-2.32	4.61
SDZ	-6.20	-1.02	5.18
PCL	-6.49	-0.50	5.99
H_2DCB	-5.82	-1.48	4.19

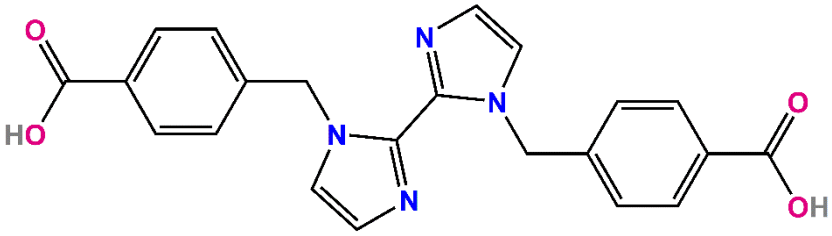

Scheme S1 Schematic drawing of the ligands H_2DCB.

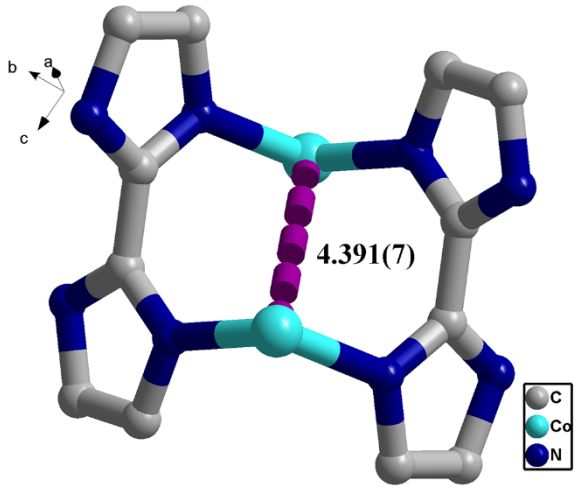

Figure S1 The binuclear [Co_2(biimidazole)$_2$] unit in **1**.

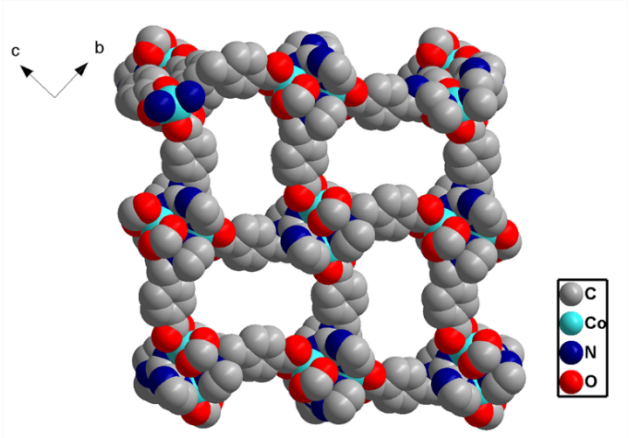

Figure S2 The 3D framework with 1D channels in **1**.

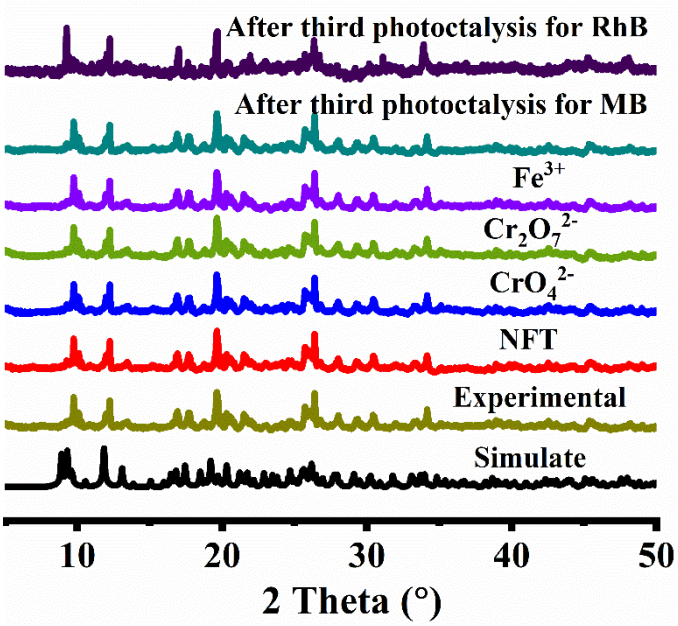

Figure S3 The PXRD patterns for **1** under different conditions.

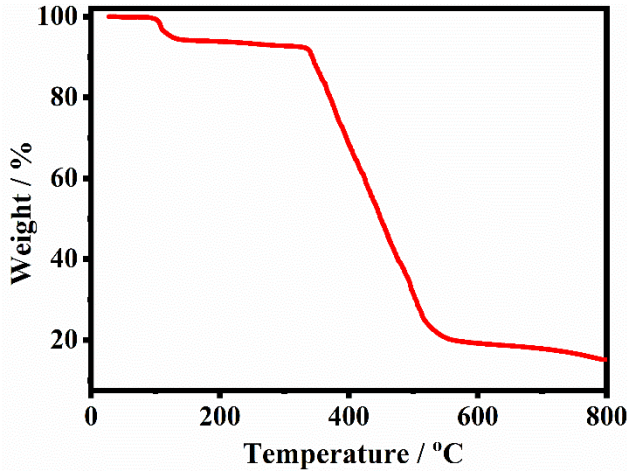

Figure S4 The TG curve of **1**.

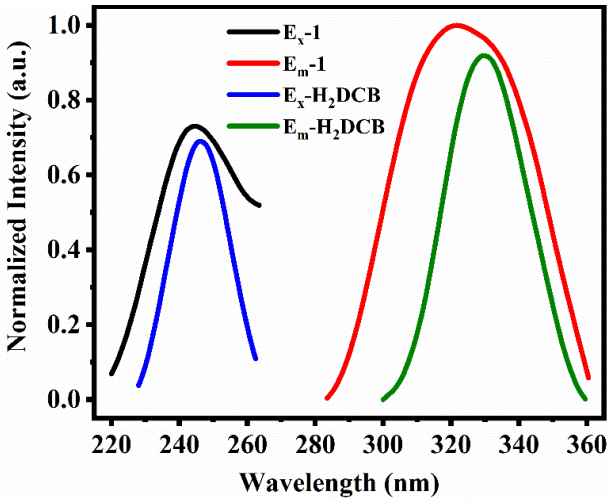

Figure S5 The solid state fluorescent excitation and emission spectra for **1** and H_2DCB.

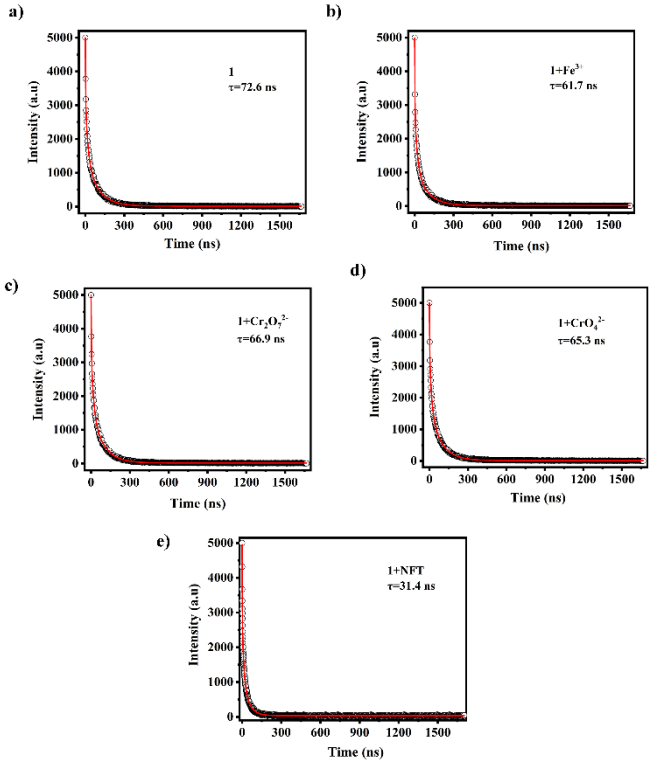

Figure S6 Experimental and fitting lifetime curves of the suspension of **1** (a) before and after addition of Fe^{3+}(b), $Cr_2O_7^{2-}$(c), CrO_4^{2-}(d) and NFT(e) (λ_{ex} = 245 nm).

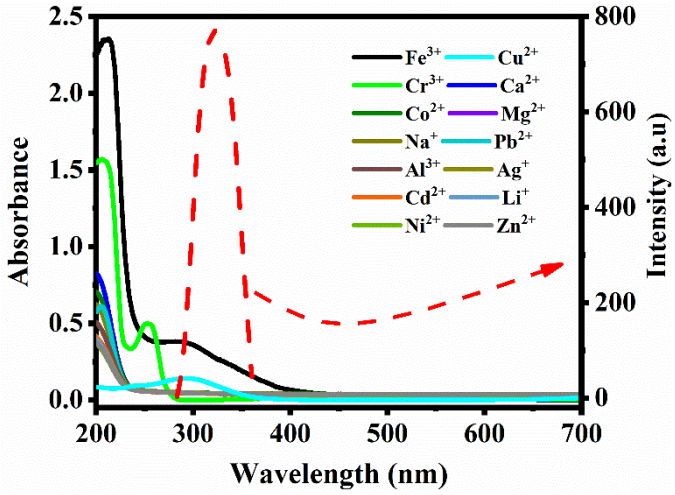

Figure S7 UV-vis spectra of different metal cations and the emission spectra of **1** (red) in H_2O solution.

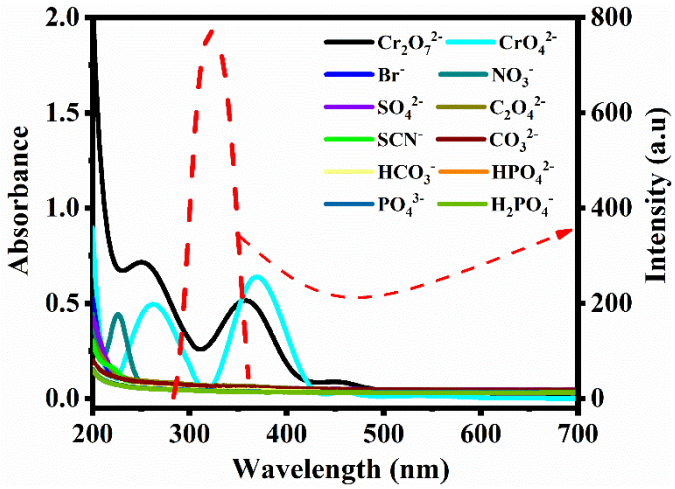

Figure S8 UV-vis spectra of different anions and the emission spectra of **1** (red) in H_2O solution.

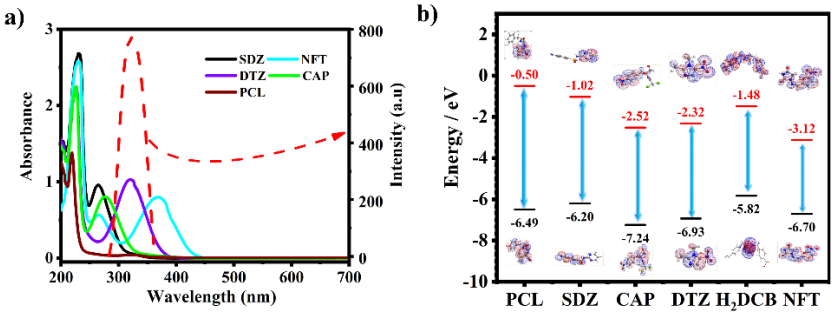

Figure S9 (a) UV-vis spectra of different antibiotics and the emission spectra of **1** (red) in H_2O solution; (b) The HOMO and LUMO energy levels for different antibiotics and H_2DCB ligand.

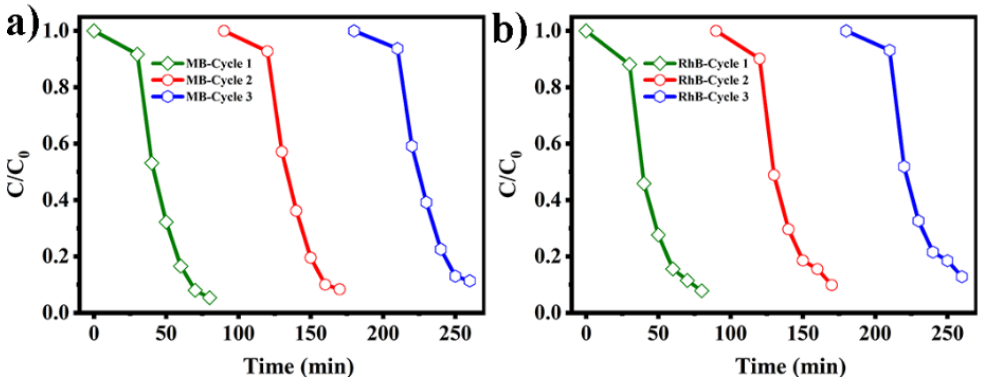

Figure S10 Cycling runs of **1** for the degradation of MB(a) and RhB(b).

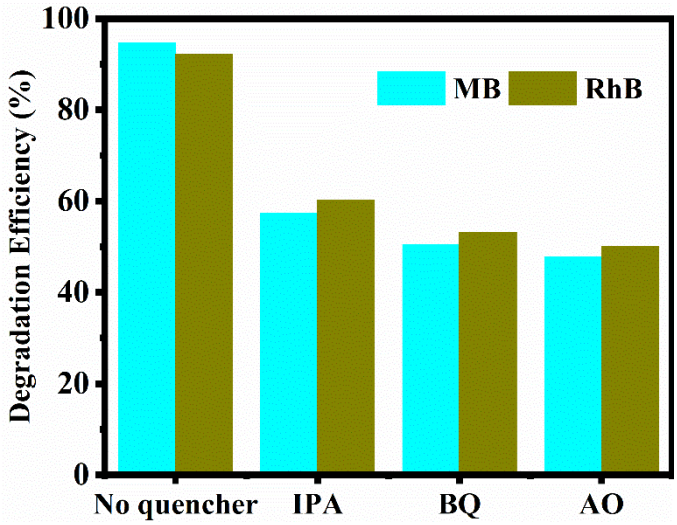

Figure S11 Trapping experiment of active species during the photocatalytic reaction with **1**.